Summer Internship Project
Report

Modeling the process of photosynthesis in leaf cells images

Submitted by

Yannis Sauzeau
yannis.sauzeau@etu.univ-poitiers.fr
University of Poitiers

Under the guidance of

Jiří Hladůvka
jiri@prip.tuwien.ac.at
Walter G. Kropatsch
krw@prip.tuwien.ac.at
Thierry Urruty
thierry.urruty@univ-poitiers.fr

TU Wien
Faculty of Informatics
Institute of Visual Computing and Human-Centered Technology
Pattern Recognition and Image Processing Group
Favoritenstr. 9/5. Stock/Stiege 2/E193-03
A-1040 Vienna, Austria

Abstract

This internship report contains the results of 3 months of internship in the Pattern Recognition and Image Processing Group at the Vienna University of Technology. After an introduction presenting the laboratory, the research project and a technical overview of the internship, we present the work done and the results obtained. A big part of the report is focus on the main research topic, which is the modelling of the diffusion of CO_2 in the leaf cells. The future work will be focused on the continuation of the research and on the absorption of CO_2 by the leaf cells in order to achieve the objective of the project. A conclusion is given on the diffusion of CO_2 in the leaf cells with a paper written for a workshop on the topic.

Contents

Chapter 1

Objective

This internship had several personal objectives:

- Discover the world of research in the field of computer vision in a scientific way.
- Put into practice my knowledges acquired during my bachelor and my first year of master.
- Develop my english skills in order to be able to communicate with the world of research.

The technical objective of the internship was to contribute to an interdisciplinary research project bridging plant biology, 3D imaging, and computer science. The objective of this project is to make a collaboration between the plant biologists and the computer scientists in order to understand better the biological processes involved in the photosynthesis of the plant. With this understanding, we will be able to reduce the amount of water we give to the plant for the growing process.

Chapter 2

Introduction

2.1 PRIP Laboratory

2.1.1 Presentation

The Pattern Recognition and Image Processing Laboratory (PRIP) is a research group of the Vienna University of Technology (TU Wien) and is part of the Computer Science department. The TU Wien is Austria's largest research and educational institution in the field of technology and natural sciences. The Computer Science department is one of Europe's leading research and innovation institutions. PRIP Laboratory is focused on advanced image representations and methods that allow the structure of the image to become an essential part of recognition systems. Among the people working in the PRIP Laboratory are:

- Prof. Walter G. Kropatsch, Head of the Group.
- Dr. Jiří Hladůvka, My tutor.
- Majid Banaeyan, PhD student.
- Darshan Batavia, PhD student.

2.1.2 *Water's gateway to heaven* project

Water's gateway to heaven is an interdisciplinary research project funded through the Life Sciences programme on Multimodal Imaging of the Vienna Science and Technology Fund (WWTF) [9]. The project is a collaboration between three viennese universities:

- Plant ecophysiologists and anatomists at the University of Natural Resources and Life Sciences [11].
- Plant cell biologists at the University of Vienna [12].
- Computer scientists expert in pattern recognition and image analysis at the Vienna University of Technology (TU Wien) [13].

The project focusses on the stomata, tiny pores on the surface of plant leaves. Stomata open and close to provide CO_2 for photosynthesis and to limit water loss. This project uses novel temporal $3D$ imaging to provide a better description of stomatal movements in order to get a mechanistic understanding of how transient this movement. The goal is to answer long-standing questions about stomatal movements and to generate basic knowledge on how to improve stomatal responses under dynamic environments in order to increase net productivity and water-use efficiency [15].

2.2 Technical overview

The images use for this project are $3D$ images of leaves coming from high-resolution X-ray micro-tomography (micro-CT) and fluorescence microscopy. The size of the images is $2000 \times 2000 \times 2000$ pixels. In order to track the change of the individual cells over time, hierarchies of abstract topological cell complexes are used, which will reduce the image data to a neighboring structure of the plant cells without losing the relation to the original data. This makes it possible to verify hypotheses at any time that arise during the course of the biological analysis but may not have been known at the time the hierarchy was built. Furthermore, this structure of the plant cells is to be used to simulate dynamic processes [14].

2.2.1 Generalized maps

The data structure chosen for this project is the n-dimensional generalized map (n-Gmap). An n-Gmap is a combinatorial data structure allowing to describe an n-dimensional orientable or nonorientable quasi-manifold with or without boundary [7]. This data structure is defined by a set of darts D on which act $n+1$ involutions α_i satisfying composition constraints of the following definition [4]:

Definition 1 (n-Gmap)**.** *An n-Gmap with $0 < n$, is an $(n+2)$-tuple $G = (D, \alpha_0, \ldots, \alpha_n)$ where:*

1. *D is a finite set of darts;*

2. $\forall i \in \{0, \ldots, n\} : \alpha_i$ *is an involution on* D*;*

3. $\forall i \in \{0, \ldots, n-2\}, \forall j \in \{i+2, \ldots, n\} : \alpha_i \circ \alpha_j$ *is an involution on* D*.*

Python implementation

For the project, PRIP has provided an implementation in Python based on the algorithms described in [7]. It consists in a hierarchy of classes which have their root in the *nGmap* class, that is an array based implementation of the gmap, where a set of arrays is used to store the involutions. The *PixelMap* class extends *nGmap* and is a 2-Gmap representing an RxC image grid. The *LabelMap* class extends *PixelMap* and adds the possibility to build a 2-Gmap representing an RxC image grid from a list of labels. This last class is very useful for the project because it allows to convert the micro-CT images into a 2-Gmap with the labels of the different leaf cells. After that we can easily make operations on this 2-Gmap and apply image processing algorithms on it.

2.2.2 Geodesic Distance Transform

The Geodesic Distance Transform (GDT) computes distances within the connected component of interest in a labeled image. The objects of interest are considered as the foreground objects and the remaining objects are considered as background. The computation of the GDT in a Gmap can be done in parallel with a logarithmic time complexity [2]. We can compute the GDT on a labeled leaf image to know the distance between the stomata and the mesophyll cells where the photosynthesis takes place. The stomata act as gates to control the amount of CO_2 that is released. The CO_2 propagates through the airspace to reach the mesophyll cells. On the figure (1) we inialized the seed label as the stomata connected component and we computed the GDT on the airspace propagation label and mesophyll cells as the target label.

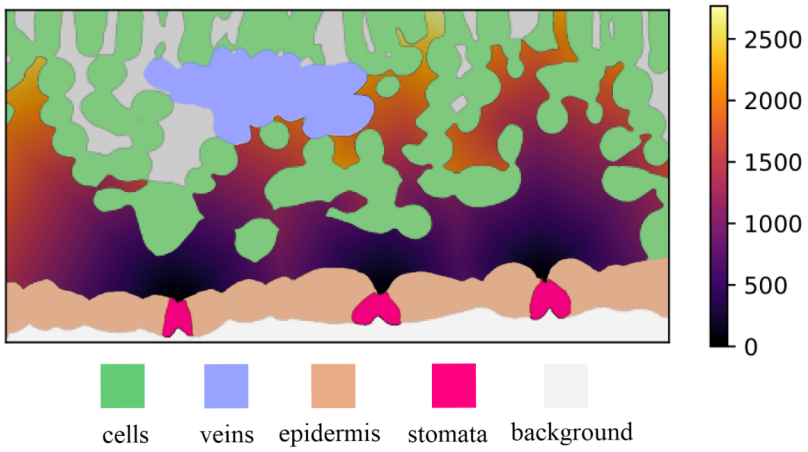

Figure 1: GDT from stomata to mesophyll cells through the airspace

Chapter 3

Work Done

3.1 First work

During the first month, my work was mainly focused on being familiar with the project and the data, in order to find the best way to contribute to the project.

3.1.1 Python library

Carmine Carratù, the previous ERASMUS student, has been working on algorithms for the computation of distance transform into n-Gmaps. My goal was to understand the code and know how to use it to create figures for future publications. The code was not documented so in reading the code I started to comment it and create documentation. I also bring some optimizations to the code. Some functions was not very helpful for the purpose of the project and the code was in several files, whereas we wanted to keep the code as simple as possible in one notebook. So I created this notebook to combine all the usefful and documented functions in one place.

New representation on a n-Gmap

The representation of the distance transform was changed to be more intuitive. On the figure (2a) the distance transform is represented as a n-Gmap with the distance values on the dart. It's hard to see the variation of the distance values. The new representation is shown in the figure (2b). This representation uses triangles for each dart showing the distance values. In addition, we use the *inferno* color map that is perceptually uniform with monotonically increasing luminance [8].

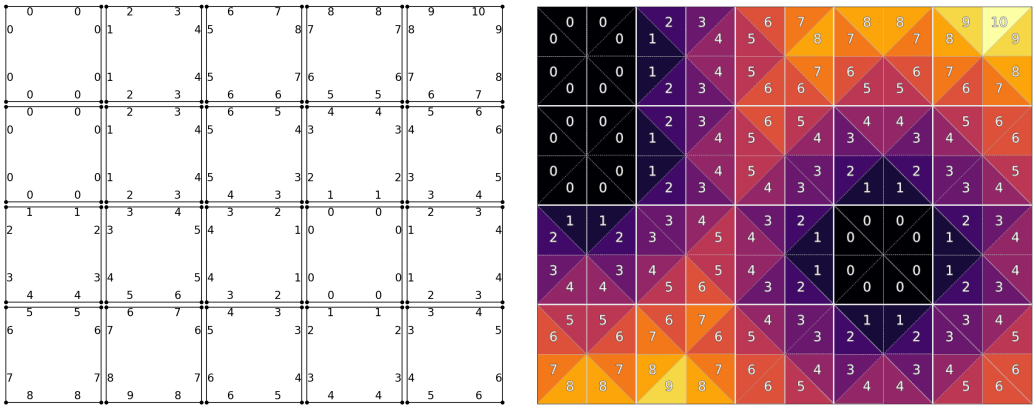

(a) Old representation **(b)** New representation

Figure 2: Different representations of the distance transform on a n-Gmap

New representation on a leaf image

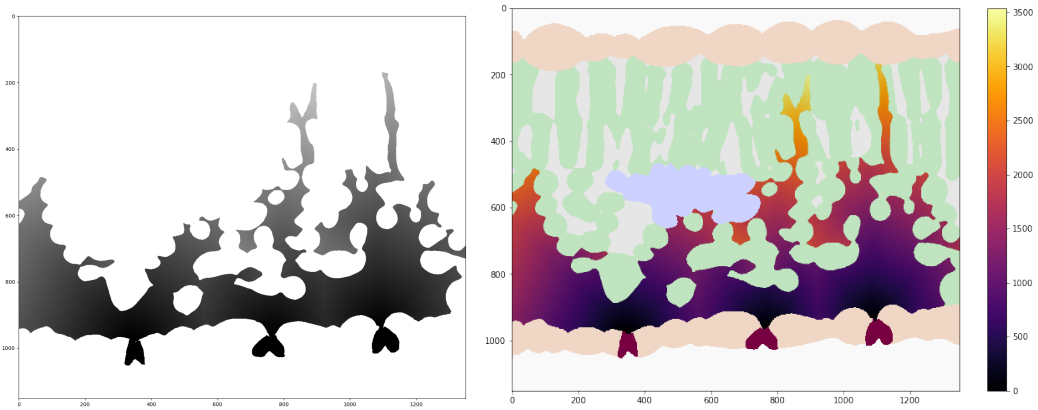

(a) Old representation **(b)** New representation

Figure 3: Different representations of the distance transform on a leaf

On the leaf image, the representation was changed too. Before the distance transform was print with a black and grey color map as shown in the figure (3a). The new representation, shown in the figure (3b) uses the *inferno* color map and an overlay can be seen to show the other parts of the leaf image.

```
PS C:\Users\Yannis Sauzeau\Documents\combinatorial\combinatorial> python .\command_lines.py --help
Usage: command_lines.py [OPTIONS]

  Command line interface for plotting images.

Options:
  -p, --path FILE             Path to the image  [required]
  -o, --output FILE           Output path  [default: output.gif; required]
  -s, --seeds INTEGER         Seed label  [required]
  -v, --verbose               Verbose mode
  -f, --frame INTEGER         Frame number
  -i, --interval INTEGER      Interval between frames (ms)  [default: 100]
  -t, --triangle              Draw triangle on each label
  -pg, --propagation INTEGER  Propagation label
  -tg, --target INTEGER       Target label
  -c, --colormap TEXT         Colormap  [default: inferno]
  -ol, --overlay              Overlay mode
  -l, --legend                Display legend
  -a, --axis                  Display axis
  --title TEXT                Display title
  --help                      Show this message and exit.
```

Figure 4: Command line program for wave propagation animation

Wave propagation animation

The distance transform algorithm uses a wave propagation method to propagate the distance values. I used *Click* [3] Python package to create a command line program that can be used to animate the propagation of the distance transform. On the figure (4) the different options for the command line program are shown. Among this options, we have the required integer for the seed label, it's form the pixel with this label that the wave will start propagating. The propagation label integer corresponds to the pixel with this label that the wave will propagate to, and the target label integer is the same but for the target pixel.

3.1.2 Diffusion equation

In order to achieve the main goal of the Watergate project it's important to study the gas exchange process that occurs in plant leaves. The distance transform is used to compute the geodesic distance from stomata to mesophyll cells where the photosynthesis is performed. The gas exchange rate depends on this distance over which the diffusion occurs [10]. To study gas exchanges inside leaves, we have chosen the diffusion equation, described in 2D by this Partial Differential Equation (PDE):

$$\frac{\partial u}{\partial t} = \alpha \left(\frac{\partial^2 u}{\partial x^2} + \frac{\partial^2 u}{\partial y^2} \right) \tag{3.1}$$

where $u(x, y, t)$ is the concentration at position x, y in time t and α is the diffusion coefficient.

Iterative solution

With a finite-difference method, we can convert the PDE (3.1) into an explicit equation described as follows:

$$u(x,y,t+1) = u(x,y,t) + \alpha\big(u(x+1,y,t) + u(x-1,y,t) + u(x,y+1,t) + u(x,y-1,t) - 4u(x,y,t)\big) \quad (3.2)$$

where $\Gamma(x)$ is the set of neighbors of pixel x.

3.2 Modeling the Diffusion of CO_2 inside Leaves

3.2.1 1D Diffusion

The diffusion equation in 1D becomes

$$u(x,t+1) = u(x,t) + \alpha\big(u(x-1,t) + u(x+1,t) - 2u(x,t)\big) \quad (3.3)$$

where $t \geq 0$ is the iteration count and x the pixel index along the sequence. We assume that the total gas volumes (3.4) of both sequences does not change by the diffusion, e.g. for all iterations t.

$$\sum_x u(x,t) = \sum_x u(x,0) \quad (3.4)$$

Diffusion propagates in both directions (increase and decrease of index) symmetrically. Consequently we have for all iterations before reaching the end of the sequence:

$$u(x,t) + u(y,t) = L + H \quad \text{for all } x + y = 1 \quad (3.5)$$

Sequence initialization

Consider one 1D sequence of 2-connected pixels without self-intersection. Let's note x the index along the sequence and $u(x,t)$ the concentration at the time t. The first half ($x \leq 0$) should be filled with a high concentration of CO_2, H, and the second half ($x > 0$) with low concentration of CO_2, L:

x	...	-3	-2	-1	0	1	2	3	4	...
$u(x,0)$	...	H	H	H	H	L	L	L	L	...

Table 1: Sequence initialization

x	...	-3	-2	-1	0	1	2	3	4	...
0	...	H	H	H	H	L	L	L	L	...
1	...	H	H	H	L	H	L	L	L	...
2	...	H	H	L	$2H-L$	$2L-H$	H	L	L	...
3	...	H	L	$3H-2L$	$4L-3H$	$4H-3L$	$3L-2H$	H	L	...

Table 2: Result with $\alpha = 1$

Normalized formula

Setting $\alpha = 1$ we notice that $u(x,t)$ starts oscillating around the boundary between L and H already at the second iteration:

The calculated values, $2H - L > H$, $2L - H < L$, are outside the interval $[L, H]$. The reason is that the differences to the center pixels need to be normalized, or equivalently the range of $\alpha \in [0, 1/2]$ in 1D. The same result with $\alpha = 1/2$:

x	...	-3	-2	-1	0	1	2	3	4	...
0	...	H	H	H	H	L	L	L	L	...
1	...	H	H	H	$\frac{H+L}{2}$	$\frac{L+H}{2}$	L	L	L	...
2	...	H	H	$\frac{3H+L}{4}$	$\frac{3H+L}{4}$	$\frac{3L+H}{4}$	$\frac{3L+H}{4}$	L	L	...
3	...	H	$\frac{7H+L}{8}$	$\frac{7H+L}{8}$	$\frac{H+L}{2}$	$\frac{L+H}{2}$	$\frac{7L+H}{8}$	$\frac{7L+H}{8}$	L	...

Table 3: Result with $\alpha = 1/2$

Notice that for $\alpha \leq 1/2$ the monotonicity of the complete sequence is preserved. The diffused values are linear combinations of L and H and remain within $[L, H]$. The diffusion could be formulated with the neighborhood $\Gamma(x)$ for all indices x as follows:

$$u(x, t+1) = u(x,t) + \frac{\alpha}{|\Gamma(x)|} \sum_{n \in \Gamma(x)} (u(n,t) - u(x,t)) \tag{3.6}$$

With this formula, α needs to be normalized to the range $[0, 1]$. This formulation would also extend to higher dimensions.

Wavefront formula

We can derive direct formula (polynomials of degree t and parameters α, x, L, H) for any iteration t without the need to do the intermediate iterations within the first wave propagation, i.e. until the front reaches the end of the sequence. A simple formula for the front of the wave is:

$$u(t,t) = (1-\alpha^t)L + \alpha^t H \tag{3.7}$$

If t is the result of the distance transform, then the value of the wavefront can be computed directly without reference to intermediate results of previous iterations.

Polynomial Basis Function

More concretely, the weights of L and H for $t = 0 \ldots 2, x = -2 \ldots 3$ can be expressed as polynomials of α:

x	$u(x,t)$		
3	L	L	L
2	L	L	$(1-\alpha^2)L + \alpha^2 H$
1	L	$(1-\alpha)L + \alpha H$	$(1-2\alpha+3\alpha^2)L + (2\alpha-3\alpha^2)H$
0	H	$(1-\alpha)H + \alpha L$	$(1-2\alpha+3\alpha^2)H + (2\alpha-3\alpha^2)L$
-1	H	H	$(1-\alpha^2)H + \alpha^2 L$
-2	H	H	H
t	0	1	2

Table 4: Weights of L and H expressed with polynomials

We observe that the coefficients L and H are symmetric with respect to $x = 0.5$ and the polynomial of L is $1-$ the polynomial of of H for $x > 0$. For $x \leq 0$, it's the opposite, i.e. the polynomial of H is $1-$ the pronominal of L:

$$\begin{aligned} u(x,t) &= \sum_{k=0}^{t} c(x,t,k)\alpha^k L + (1 - \sum_{k=0}^{t} c(x,t,k)\alpha^k)H \\ &= H - \left(\sum_{k=0}^{t} c(x,t,k)\alpha^k\right)(H-L) \end{aligned} \tag{3.8}$$

where $c(x,t,k)$ is the coefficient of the polynomial of degree k at iteration t and x is the index along the sequence.

t	0	1		2			3				4				
x \ k	0	0	1	0	1	2	0	1	2	3	0	1	2	3	4
4	1	1	0	1	0	0	1	0	0	0	1	0	0	0	-1
3	1	1	0	1	0	0	1	0	0	-1	1	0	0	-4	7
2	1	1	0	1	0	-1	1	0	-3	5	1	0	-6	20	-21
1	1	1	-1	1	-2	3	1	-3	9	-10	1	-4	18	-40	35
0	0	0	1	0	2	-3	0	3	-9	10	0	4	-18	40	-35
-1	0	0	0	0	0	1	0	0	3	-5	0	0	6	-20	21
-2	0	0	0	0	0	0	0	0	0	1	0	0	0	4	-7
-3	0	0	0	0	0	0	0	0	0	0	0	0	0	0	1

Table 5: Coefficients $c(x, t, k)$ for the very first time steps ($t = 0 \dots 4$).

Deriving the coefficients of the polynomial (Table 5 shows the coefficients for the first 4 time steps), we arrived at the following closed-form involving binomial coefficients for negative arguments[1] [6].

$$c(x, t, k) = (-1)^{1+x+k} \binom{t}{k} \binom{2k-1}{x+k-1} \tag{3.9}$$

With respect of property (3.5), we have this property:

$$\sum_{k=1}^{t} c(x, t, k)\alpha^k = -\sum_{k=1}^{t} c(y, t, k)\alpha^k \quad \text{for all } x + y = 1 \tag{3.10}$$

With the property above, to know all the values of $u(x, t)$ of a certain iteration t, we only have to compute $\sum_{k=0}^{t} c(x, t, k)\alpha^k$ with $x \in [1, t]$.

Result

To study the diffusion of CO_2 in the leaf from stomata to the leaf cells, we first compute the distance transform $d(x)$ of each pixel $x \in R$ in the airspace R. Afterward, we compute the coefficients $c(t, k, x)$ with $t = \max_{x \in R} d(x)$. Once we have the coefficients, we can compute the concentration $u(x, t)$ by (3.9). The result is identical to the iterative solution and is visualized in figure (5).

Another point of interest is to compute only the diffusion values for the pixels corresponding to the leaf cells border. Indeed, to know the concentration of the leaf cells, we don't need to compute the diffusion values for the other parts of the leaf.

[1] Explaining the colored entries in Table 5

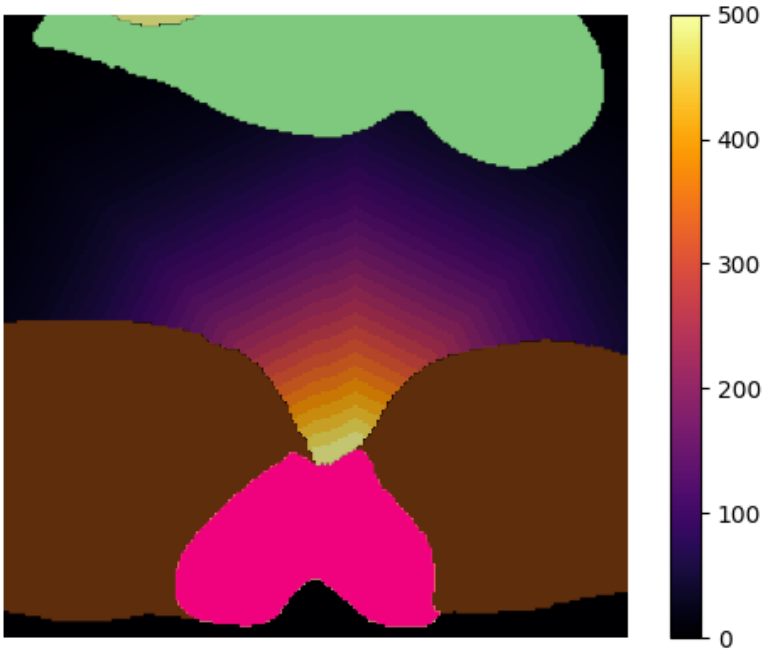

Figure 5: Equation (3.8) used to describe the diffusion of CO_2 from stoma.

3.2.2 Stomata's movement

In this section we will study the effects of the movement of the stomata. Let's start with a simple example. First, initialize a sequence like in Table 1. The size of the sequence is 20 pixels with $x \in [-9, 10]$, $H = 100\%$, $L = 0\%$ and $t = 0$ (see the figure (6a)). This sequence represents a closed stoma at the position $x = 0$, the pixels with negative index are the ones outside the leaf and the ones with positive index are the ones inside the leaf. When $t > 0$ the stoma is open. Using the iterative method (3.6) with $\alpha = 1$ we want to know the time t when the end of the sequence is near to be stabilized, i.e. that the value at the end of the sequence is greater than 49%. This value is reached at time $t = 336$ (see the figure (6b)).

Different sequence sizes

We want to know if the size of the sequence influences the time taken to reach the stabilized state. We use the same method as above but with different sizes of sequence. For 10 pixels, the stabilized state is reached at time $t = 83$, for 50 pixels at time $t = 2103$ and for 100 pixels at time $t = 8416$. With a size of 10 pixels the time taken to reach the stabilized state is much smaller than with a size of 50 pixels and with a size of 100 pixels. With the sequence

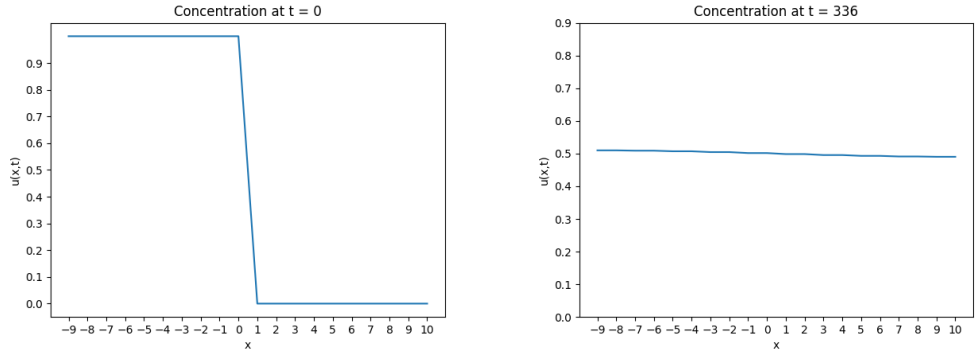

(a) $u(x, 0)$ **(b)** $u(x, 336)$

Figure 6: Concentration $u(x, t)$ in a sequence of size 20 at the initialization and near the stabilized state

of 100 pixels it takes 100 times longer to reach the stabilized state than with the sequence of 10 pixels.

Function to calculate the time taken to reach the stabilized state

The table below shows the time taken to reach the stabilized state for the first sequences from 2 to 10 pixels. The figure (7) shows this function for sequences between 2 and 100 pixels.

number of pixels in the sequence	2	3	4	5	6	7	8	9	10
time to reach the stabilized state	1	6	12	20	29	40	52	67	83

Table 6: Time to reach the stabilized state for first 8 sequences of sizes between 2 and 10 pixels

Let's see if sequence of time obtained from the table can be computed from the number of pixels. To know if the time to reach the stabilized state can be computed from the number of pixels we can see if it's a polynomial function. To that we can compute the difference table (7). We can observe that the differences didn't converge to a constant value. This is because the time to reach the stabilized state is not a polynomial function.

Stomata closing after few iterations

We want to know if the stabilized state is reached faster when the stomata close after few iterations. We start with a sequence of 100 pixels and we want to know the number of iterations needed to the end of the sequence reach

1		6		12		20		29		36	
	5		6		8		9		7		
		1		2		1		-2			
			1		-1		-3				
				-2		-2					

Table 7: Difference table for the time to reach the stabilized state for the first 5 sequences of sizes between 2 and 6 pixels

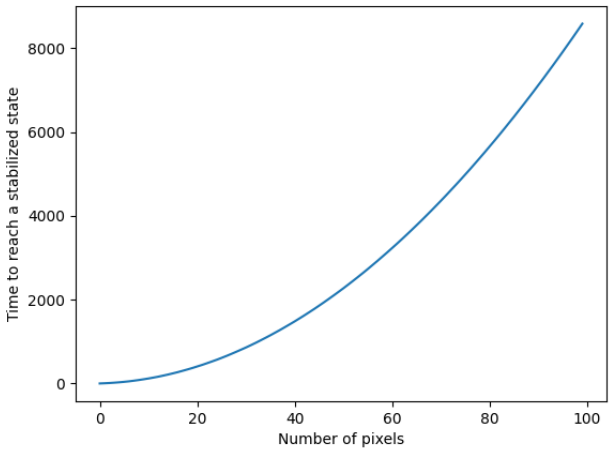

Figure 7: Function to reach a stabilized state from different sizes of sequence

the value of 25% when the stoma is always open end when the stoma close after few iterations. When the stoma is open we need time $t = 1894$ to reach the value of 25%. On the figure (8), we can see that for reaching the value of 25% the stoma need to be close after time $t = 986$. When the stoma closes at time $t = 1000$, we need $t = 4000$ to reach the value of 25%, i.e. more than two times the time needed to reach the same value when the stoma is open. More the stoma takes time to close, less we need time to reach the value of 25%. When we close the stoma at time after $t = 1650$, then the time to reach the value of 25% is constant and equal to $t = 1894$.

3.2.3 Simulate the diffusion problem for higher dimensions

Let's transform our 1D sequence into a 2D sequence. We can do this by creating a matrix with the same size as the 1D sequence and filling it with the values of the 1D sequence. Let's note x the index of the pixel in the

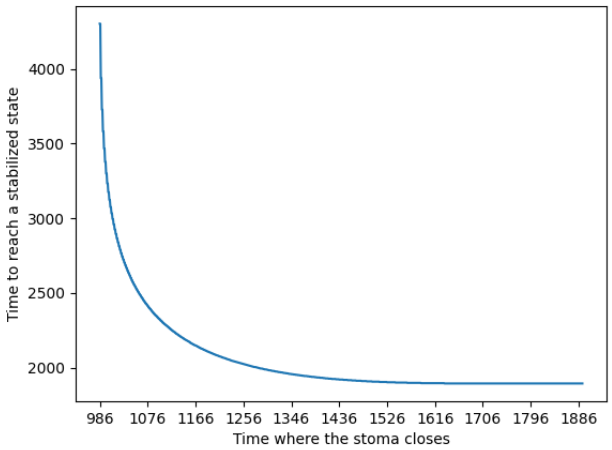

Figure 8: Function to reach a stabilized state when the stoma closes after x iterations

1D sequence and y the index of the pixel in the 2D sequence, and $u(x, y, t)$ the concentration at the iteration t. To differentiate the notation between the diffusion in the 1D and 2D case, we will use $u_{1D}(x, t)$ for the 1D diffusion and $u_{2D}(x, y, t)$ for the 2D diffusion. We will initialize the matrix with $u_{2D}(x, y, 0) = u_{1D}(x, 0)$ like the table below:

$u(x,0,0)$	...	H	H	H	H	L	L	L	L	...
$u(x,1,0)$	...	H	H	H	H	L	L	L	L	...
$u(x,2,0)$	...	H	H	H	H	L	L	L	L	...
...	...	...	...	...	...	...	...	...	...	...
$u(x,y,0)$	...	H	H	H	H	L	L	L	L	...
x	...	-3	-2	-1	0	1	2	3	4	...

Table 8: 2D sequence initialization

2D formula idealistic model

Let's adapt the formula (3.6) to the 2D diffusion problem:

$$u_{2D}(x, y, t+1) = u_{2D}(x, y, t) + \frac{\alpha}{|\Gamma(x, y)|} \sum_{n,m \in \Gamma(x,y)} (u_{2D}(n, m, t) - u_{2D}(x, y, t)) \tag{3.11}$$

With $\Gamma(x, y)$ the set of all the pixels that are connected to the pixel (x, y). Now we can compute the diffusion for the 2D sequence and compare the results with the 1D sequence. For the computation we will take $\alpha = 1$ and $t = 100$. The results (figure (9)) show that with the same alpha, the diffusion is two time faster in the 1D sequence than in the 2D sequence. It's understandable since the 1D diffusion only propagate in two directions and the 2D diffusion propagate in four directions. When we compare the results of the first iterations in the 1D and 2D sequences with the table (3) in 1D and table (9) in 2D, we can see similarity. For instance, $u_{2D}(1, y, 1) = u_{1D}(2, 2)$, $u_{2D}(1, y, 2) = u_{1D}(2, 4)$, or $u_{2D}(2, y, 2) = u_{1D}(4, 4)$. We can generalize by the formula:

$$u_{2D}(x, y, t) = u_{1D}(2x, 2t) \tag{3.12}$$

The formula below is working only with specific conditions, i.e. $u_{2D}(x, y, 0) = u_{1D}(x, 0)$ and $u_{2D}(x, y - 1, t) = u_{2D}(x, y, t) = u_{2D}(x, y + 1, t)$.

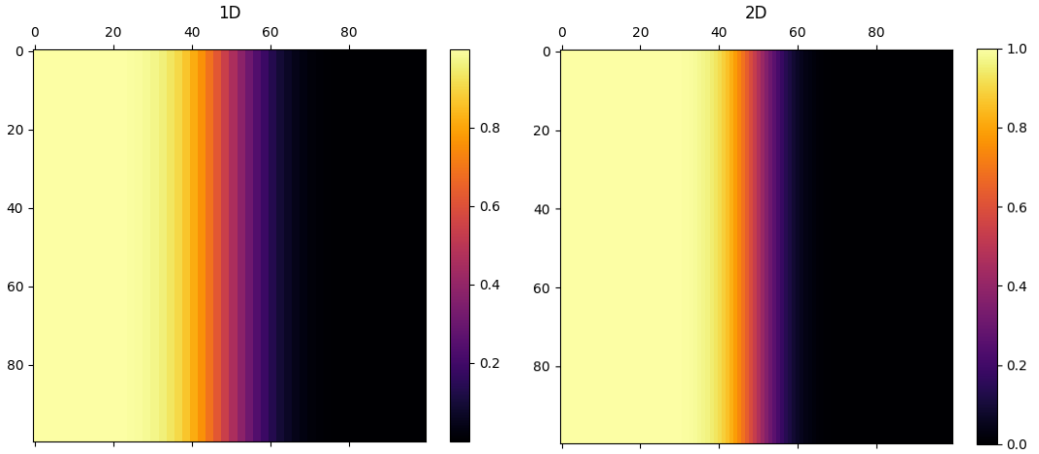

(a) Diffusion with $\alpha = 1$ in 1D sequence of size 100

(b) Diffusion with $\alpha = 1$ in 2D sequence of size 100×100

Figure 9: Diffusion with $\alpha = 1$ in 1D and 2D sequence of size 100×100

General 2D formula

The shape of stomata is like a funnel, so let's create a 2D sequence of size 100×100 that looks like a funnel. The figure (10a) shows the initial sequence. Here the formula (3.12) is not working, but we can find a formula that works for every pixel. Let's start some observations. On the first step for the 1D diffusion we can isolate two different configurations that makes changes in

x	$\dots$	-2	-1	0	1	2	3	$\dots$
$u(x,y,0)$	$\dots$	H	H	H	L	L	L	$\dots$
$u(x,y,1)$	$\dots$	H	H	$\frac{3H+L}{4}$	$\frac{3L+H}{4}$	L	L	$\dots$
$u(x,y,2)$	$\dots$	H	$\frac{15H+L}{16}$	$\frac{11H+5L}{16}$	$\frac{11L+5H}{16}$	$\frac{15L+H}{16}$	L	$\dots$

Table 9: Result with $\alpha = 1$ in 2D sequence

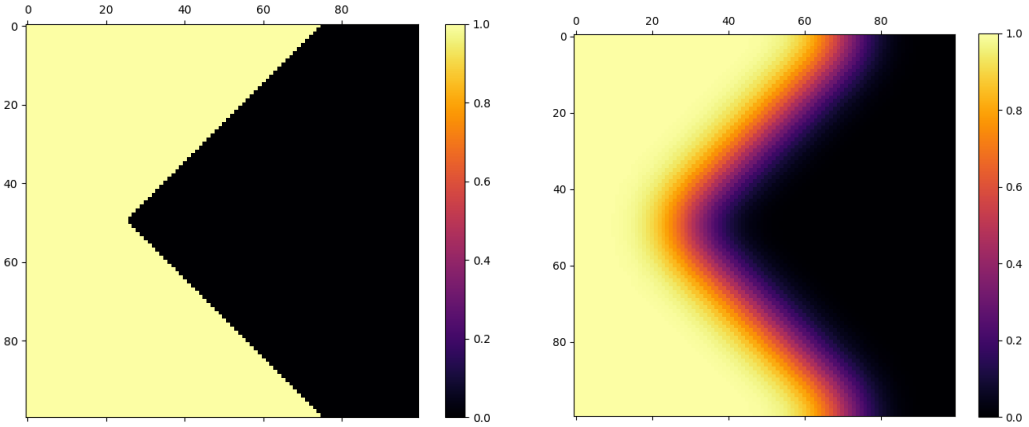

(a) 2D funnel sequence at the initialization

(b) Diffusion with $\alpha = 1$ in 2D funnel sequence at iteration 100

Figure 10: Diffusion in 2D sequence of size 100×100 more near the stomata shape

the sequence. Each of this configuration leads to four variations in the 2D sequence:

- First configuration when $u(x,0) = H$ (figure (11a)):

  In this configuration in 1D, the value at $t = 1$ is different of the value at $t = 0$, only if one of the neighbor is H and the other is L. If both neighbors are H the value at $t = 1$ is the same of the value at $t = 0$. Taking in consideration the case when $u(x,0) \neq u(x,1)$, we want to know the similarity between the 1D and 2D sequences. In the figure (11a) we can see that the 1D sequence can be represented as four 2D sequences whose two sequences has the same number of neighbors H and L. So we will defined the similarities between the 1D and 2D. Let's defined N_H and N_L as the number of neighbors H and L in the 2D sequence. Let's note the subtraction between N_H and N_L as $\Delta_{HL} = N_H - N_L$. Then the formula is:

$$u_{2D}(x, y, t) = u_{1D}(\Delta_{HL}x, |\Delta_{HL}|t) \tag{3.13}$$

- Second configuration when $u(x, 0) = L$ (figure (11b)):

  The observations are the same as the first configuration, but we need to subtract N_L from N_H to get the correct value. Let's note this subtraction as $\Delta_{LH} = N_L - N_H$. Then the formula is:

$$u_{2D}(x, y, t) = u_{1D}(\Delta_{LH}x, |\Delta_{LH}|t) \tag{3.14}$$

2D formula using the 1D formula

To summarize, we can find a formula to compute the value of concentration $u_{2D}(x, y, t)$ in the 2D sequence with the value of concentration $u_{1D}(x, t)$ in the 1D sequence. The formula can be written as:

$$u_{2D}(x, y, t) = u_{1D}(\Delta_N x, |\Delta_N|t) \text{ where } \Delta_N = \begin{cases} \Delta_{HL} & \text{if } u_{1D}(x, 0) = H \\ \Delta_{LH} & \text{if } u_{1D}(x, 0) = L \end{cases} \tag{3.15}$$

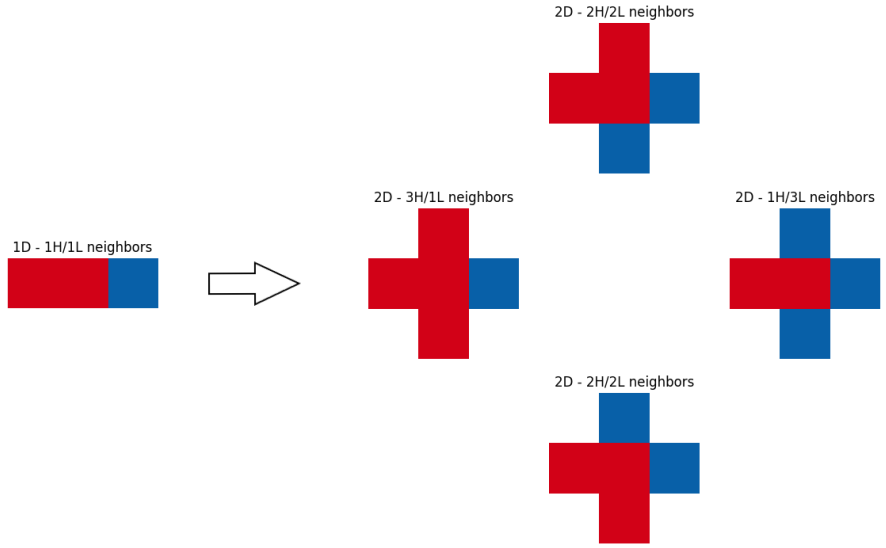

(a) HHL 1D sequence to 2D sequence

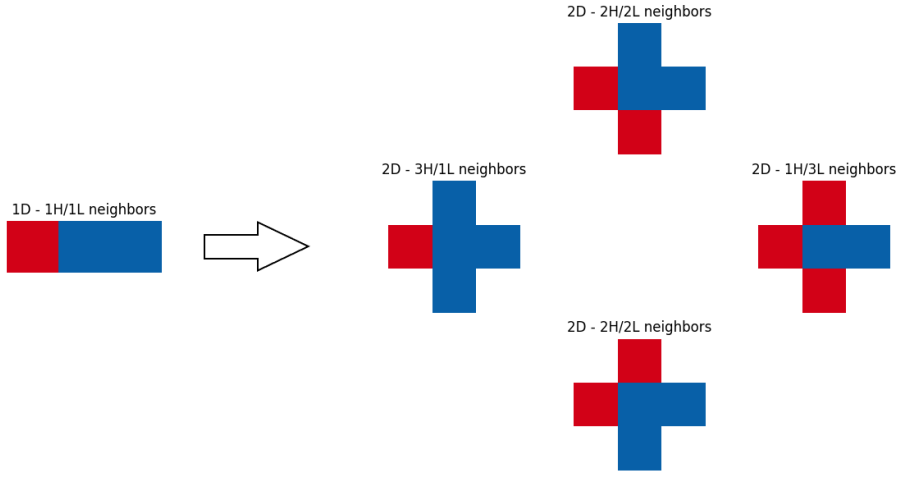

(b) HLL 1D sequence to 2D sequence

Figure 11: From initial 1D sequence to 2D sequence

Chapter 4

Future Work

4.1 Back-propagation of reflected wave

When the propagation will reach the end of the sequence, a reflected wave will be propagated back to the beginning of the sequence. As a consequence the two extrema get closer to each other to reach the stabilized state. If we take a sequence of L with N elements, the end of the sequence is reached after N steps. We know the value of the wavefront when the end of the sequence is reached and just before the back propagation. We want to know the value of this wavefront when the back propagation starts. Using the equations (3.6) and (3.7) we can compute this value:

$$\begin{aligned} u(N, N+1) &= u(N, N) + \alpha \left(u(N-1, N) - u(N, N)\right) \\ &= (1-\alpha)u(N, N) + \alpha \times u(N-1, N) \\ &= (1-\alpha)((1-\alpha^N)L + \alpha^N H) + \alpha \times u(N-1, N) \end{aligned} \tag{4.1}$$

If $\alpha = 1$ then $u(N, N+1) = \alpha \times u(N-1, N)$

Assumption to verify

We have the assumption that the back propagation at the end of the sequence is like a flip of the start of the sequence. The concentration stays the same in the sequence during the time (property (3.4)). Before the back propagation the start of the sequence is $u(-N, N) = H$ with N the size of the H sequence. At time $N+1$ the back propagation starts and the concentration start to decrease ($u(-N, N+1) < H$). While this concentration decrease the concentration at the end of the sequence is increasing ($u(N, N+1) > L$). Our assumption is that the decreasing concentration of the start of the sequence is the same as the increasing concentration of the end of the sequence.

4.2 Absorption of CO_2 by the cells

According to the article [1], the CO_2 flux in the leaf cells is influenced by several factors:

- Light
- Temperature
- Ambient CO_2 concentration
- Photosynthetic capacity of the mesophyll cells
- Size of the stoma opening
- Leaf structure
- Diffusion coefficients in the different parts

The CO_2 concentration distribution is a continous sink and relatively constant over the airspace, but decrease rapidly in the mesophyll cells. Concentration inside the cells did not decrease more than 18% from the value in the airspace. The article [5] says that the CO_2 diffusion can be variable in short time range, but it's a physical process dependant of structure so the diffusion rate is constant for time ranges of hours. This mecanism of CO_2 diffusion is a matter of controversy vivid debate in the scientific community.

Minimal model

Consider a 1D sequence like on the section 3.2.2. We will use the same sequence of size 100 pixels but this time the end of the sequence will absorb CO_2 and the rest of the sequence will diffuse it. We will assume that the diffusion is decrease by 10% in the mesophyll cells. In our sequence the ten last pixels will be the mesophyll cells. The formula for the diffusion does not change, but the diffusion rate is different. Indeed, the diffusion coefficient is different for the mesophyll cells pixels than for the rest of the sequence, it's equal to $0.9 \times \alpha$. With this rate of absorption by the mesophyll cells, we need $t = 10236$ to obtain a concentration of 49% instead of $t = 8416$ without absorption. It takes 21% more time to reach the stabilized state with 10% absorption than without absorption.

Effect of absorption on stabilized concentration

Because of the absorption phenomena the assumption (3.4) is not true anymore. If the absorption is too high, the concentration will decrease too fast and the sequence will not reach the value of 49%. For the sequence of 100 pixels, when the absorption is greater than 16% the concentration at the end of the sequence will be less than 49%. We want to plot the time taken to reach the value of 49% at the end of the sequence for the different values of the absorption (see figure (12)). We can see that the absorption influences a lot the time to reach a state near the stabilized state.

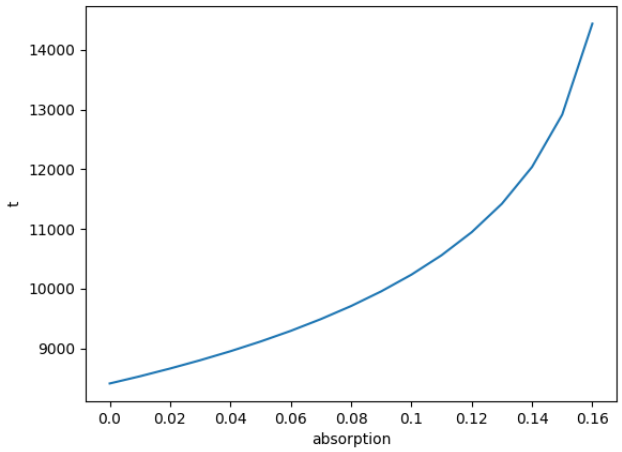

Figure 12: Time to reach the value of 49% at the end of the sequence for different values of absorption

Chapter 5

Conclusion

To conclude, this internship was a great opportunity to learn about the research process and to get a taste of what it is like to work in a research group. I have learned a lot about the research process and about the different tools that are used in. I have also learned a lot about research that are done in the field of computer vision, pattern recognition, and some other areas that are interesting to me. During this internship, I wrote my first scientific paper for a workshop organized by the Austrian Association for Pattern Recognition (OAGM) [16]. Currently, I don't know yet if the paper is accepted or not, but I prepared a poster for the workshop if the paper is accepted. It was a very good experience to write a paper and a poster, and I hope I could participate to the workshop if the paper is accepted.

Acknowledgment

I'm extremely grateful to Walter G. Kropatsch for giving me the opportunity to make this internship in the PRIP laboratory. I would also like to thank him for his passion for research and the way he has transmitted it. I'd like to express my deepest thanks to Jiří Hladůvka who was my supervisor during the internship. He gave me a lot of good advice and helped me to understand the research process. I would also like to thank Majid Banaeyan and Darshan Batavia for their help and support during the internship. I would like to pay my special regards to Samuel Peltier for giving me the contact of the PRIP laboratory. I must also thank Thierry Urruty my supervisor in France. Finally, I would like to thank all the people I have met during the internship and the friends I have made in Vienna.

References

[1] T. Aalto and E. Juurola. A three-dimensional model of co2 transport in airspaces and mesophyll cells of a silver birch leaf. *Plant, Cell & Environment*, 25(11):1399–1409, 2002, https://onlinelibrary.wiley.com/doi/pdf/10.1046/j.0016-8025.2002.00906.x. doi:https://doi.org/10.1046/j.0016-8025.2002.00906.x.

[2] M. Banaeyan, C. Carratù, W. G. Kropatsch, and J. Hladůvka. Fast distance transforms in graphs and in gmaps. In *IAPR Joint International Workshops on Statistical Techniques in Pattern Recognition (SPR 2022) and Structural and Syntactic Pattern Recognition (SSPR 2022), Montreal, Canada, August 26-27, 2022*, page in print, 2022.

[3] Click Python Package website. `https://click.palletsprojects.com/`.

[4] G. Damiand and P. Lienhardt. *Combinatorial Maps: Efficient Data Structures for Computer Graphics and Image Processing*. 09 2014. doi:10.1201/b17403.

[5] R. Kaldenhoff. Mechanisms underlying co2 diffusion in leaves. *Current Opinion in Plant Biology*, 15(3):276–281, 2012. doi:https://doi.org/10.1016/j.pbi.2012.01.011.

[6] M. J. Kronenburg. The binomial coefficient for negative arguments, 2011. doi:10.48550/ARXIV.1105.3689.

[7] P. Lienhardt. Topological models for boundary representation: a comparison with n-dimensional generalized maps. *Computer-Aided Design*, 23(1):59–82, 1991. doi:https://doi.org/10.1016/0010-4485(91)90082-8.

[8] K. Moreland. Why we use bad color maps and what you can do about it. *Electronic Imaging*, 2016:1–6, 02 2016. doi:10.2352/ISSN.2470-1173.2016.16.HVEI-133.

[9] Multimodal Imaging of the Vienna Science and Technology Fund website. https://www.wwtf.at/.

[10] Royal society of biology. Gas exchange. https://www.rsb.org.uk/images/12_Gas_exchange.pdf/.

[11] University of Natural Resources and Life Sciences website. https://boku.ac.at/.

[12] University of Vienna website. https://www.univie.ac.at/en/.

[13] Vienna University of Technology website. https://www.tuwien.at/.

[14] Water's gateway to heaven at PRIP website. https://www.prip.tuwien.ac.at/research/current_projects/wgh/.

[15] Water's gateway to heaven website. https://waters-gateway.boku.ac.at/.

[16] Workshop OAGM website. https://workshops.aapr.at/.

List of Figures

List of Tables